ISSN 1063-7737, Astronomy Letters, 2013, Vol. 39, No. 5, pp. 347–356. © Pleiades Publishing, Inc., 2013.
Original Russian Text © A.P. Titarenko, T.A. Ryabchikova, O.P. Kochukho, V.V. Tsymbal, 2013, published in Pis'ma v Astronomicheskiĭ Zhurnal, 2013, Vol. 39, No. 5, pp. 390–400.

Chemical Composition and Evolutionary Status of the Ap Star HD 138633

A. P. Titarenko[1,2*], T. A. Ryabchikova[2], O. P. Kochukhov[3], and V. V. Tsymbal[4]

[1] *Department of Astronomy, Faculty of Physics, Moscow State University, Moscow, 119991 Russia*
[2] *Institute of Astronomy, Russian Academy of Sciences, ul. Pyatnitskaya 48, Moscow, 119017 Russia*
[3] *Department of Astronomy and Space Physics, Uppsala University, Box 515, 751-20 Uppsala, Sweden*
[4] *Faculty of Physics, Taurida National University, pr. Vernadskogo 4, Simferopol, 95007 Ukraine*

Received December 7, 2012

Abstract—We present the results of our study of the atmospheric chemical composition and evolutionary status for the chemically peculiar Ap star HD 138633. In contrast to ordinary Ap stars that exhibit strong lines of rare-earth elements in their spectra, these elements are represented very poorly in the spectrum of HD 138633. The magnetic field is estimated to be less than 700 G, which is also atypical of peculiar Ap stars. We have detected a stratification of such elements as Fe, Si, Ca, and Y in the atmosphere of HD 138633 whose pattern agrees qualitatively with the predictions of the theory of diffusive separation of elements under the joint action of gravity and radiation pressure forces. The nonuniform distribution obtained by assuming a stepwise distribution of elements in depth agrees qualitatively with the stratification distribution for β CrB. The search for pulsations points to the possible existence of low-amplitude pulsations with a period of about 17 min.

DOI: 10.1134/S1063773713050058

Keywords: *stars—chemically peculiar stars, chemical composition, atmospheric pulsations, magnetic field.*

INTRODUCTION

HD 138633 is a representative of the group of chemically peculiar Ap stars. It was first classified in the catalog by Renson and Manfroid (2009) as Sr–Cr–Eu of type F0. HD 138633 fell into in the list for pulsation observations based on its Strömgren photometric indices (the 072.D-0138(A) program of observations on the 8-m VLT telescope), but no pulsations were detected. The star was also observed from the STEREO/HI-1A and STEREO/HI-1B satellites for rotationally induced variability. The list of observations included 1028 stars from the Renson–Manfroid catalog; objects with established or suspected membership in the class of chemically peculiar stars enter into the latter. Over 40 days of observations with a break for 20 days, HD 138633 showed no such variability (Wraight et al. 2012). Table 1 gives the basic data on HD 138633 known to date taken from Wraight et al. (2012). No other observations of HD 138633 to investigate its chemical composition and magnetic field have been carried out so far.

We took an interest in HD 138633 precisely because no pulsations were found in its atmosphere, although the Strömgren photometric indices suggest that the star falls into the observed instability strip of Ap stars. Therefore, we decided to perform a detailed analysis of the stellar atmosphere from the viewpoint of atmospheric parameters and chemical composition using currently available atomic data, model atmospheres, and codes for computing theoretical spectra as well as to establish the evolutionary status and to analyze more carefully the radial velocity pulsations in the atmosphere.

This paper is structured as follows. In Section 1, we describe the observational data and present the reduction procedures. The atmospheric parameters, magnetic field, and rotational velocity of the star are determined in Section 2. The chemical composition and the results of our stratification analysis of its atmosphere are considered in Section 3. In Section 4, we determine the evolutionary status of HD 138633 and perform a pulsation analysis.

1. SPECTROSCOPIC OBSERVATIONS AND THEIR REDUCTION

For our abundance analysis of the star, we used the averaged spectra obtained on the ESO VLT telescope with the UVES instrument to find pulsations

*E-mail: 2chlaidze@gmail.com

Table 1. STEREO observational data for HD 138633

Name	#R09	Right ascension	Declination	Apparent magnitude	Spectral type	Peculiarity class	Ann.
HD 138633	39460	233.39200	−11.06520	8.63	F0(Sr,Eu,Cr)	CP2	C

according to the 072.D-0138(A) program and taken from the European Southern Observatory archive. A total of 111 high-resolution ($\lambda/\Delta\lambda \approx 110\,000$) spectra in the range 4960–6990 Å were obtained during the monitoring. The observations cover all of this range except the region 100 Å in width near 6000 Å. All spectra passed a primary reduction (constructing an averaged bias image with its subtraction from all spectra of the flat field, the star, and the calibration lamp, correcting the images for nonuniform detector pixel sensitivity, and extracting the 1D spectra). To increase the signal-to-noise ratio, we added the spectra and performed the global continuum normalization by successively applying smoothing functions (splines) to the highest points in the corresponding spectral regions. The resulting averaged spectrum was used here. The continuum in the individual spectra was normalized using the averaged spectrum.

2. DETERMINATION OF ATMOSPHERIC PARAMETERS FOR THE STAR

Effective Temperature and Surface Gravity

Using the observed Strömgren and Geneva photometric indices, we estimated the effective temperature and surface gravity for HD 138633. The Strömgren indices ($V = 8.63$, $b - y = 0.243$, $m_1 = 0.160$, $c_1 = 1.019$, $\beta = 2.875$) were taken from the catalogue by Hauck and Mermilliod (1998). Based on the calibrations of $[b - y]$ and $[c_1]$ (Napiwotzki et al. 1993), we derived the effective temperature $T_{\rm eff} = 9351$ K and surface gravity $\log g = 4.26$. Since they dropped out of the series of remaining determinations, we disregarded these data in the averaging. The calibrations of the Strömgren indices implemented in the TempLogG software package (Kaiser 2006) are presented in Table 2. Averaging these data leads us to the following atmospheric parameters of HD 138633: $T_{\rm eff} = 8130 \pm 200$ K and $\log g = 4.02 \pm 0.14$. Unfortunately, the observed hydrogen line profiles cannot be used as an unambiguous characteristic of the effective temperature or the surface gravity in this temperature range.

Table 2. Atmospheric parameters obtained by calibrating the Strömgren photometric indices using the TempLogG code

Calibration	$T_{\rm eff}$	$\log g$	$E(b-y)$
Moon and Dworetsky (1985)	8338	4.08	0.16
Napiwotzki (1995)	9351	4.26	0.16
Balona (1994)	7931	4.15	0.16
Ribas (1997)	8308	4.04	0.16
Castelli (1997)	7946	3.82	0.16

Using the ATLAS9 code (Kurucz 1993), we computed a grid of model atmospheres with a metallicity of +0.5 for effective temperatures from 8100 to 8400 K (with a 100-K step) and surface gravities from 3.5 to 4.0 (with a 0.1 step). We then used the Synth3 code (Kochukhov 2007) to compute a series of synthetic spectra in various spectral regions. To determine the atmospheric parameters of HD 138633, we also used the data obtained below through our stratification analysis. Specifically, we calculated the distribution of Fe in two ionization stages in depth of the stellar atmosphere for the above grid of model atmospheres. For the combinations of parameters at which the deviation of the observed line profile from the synthetic one with allowance made for the nonuniform distribution was smallest, we made a detailed comparison of the observed and theoretical spectra in the range 4000–7000 Å. Taking into account the photometric data and the procedure described above, we adopted the model atmosphere with $T_{\rm eff} = 8200 \pm 100$ K and $\log g = 3.8 \pm 0.1$ as describing best the observed line profiles. Our stratification analysis is described in more detail in the corresponding section.

Magnetic Field, Rotation, and Microturbulence

Although the star is classified as Ap, HD 138633 has not been studied previously and there are no data on its magnetic field. A visual examination of the spectrum showed no visible line splitting, suggesting a small magnetic field strength. We estimated the magnetic field from the differential broadening of the Cr I 5247.56 Å line with one of the largest Lande factors, $g = 2.51$, and, at the same time, a comparatively simple triplet splitting structure. Our calculations for the Fe I 5434.52 Å line, which is insensitive to the magnetic field effect, are presented for comparison. Figure 1 compares the observed and theoretical profiles calculated without a magnetic field and in its

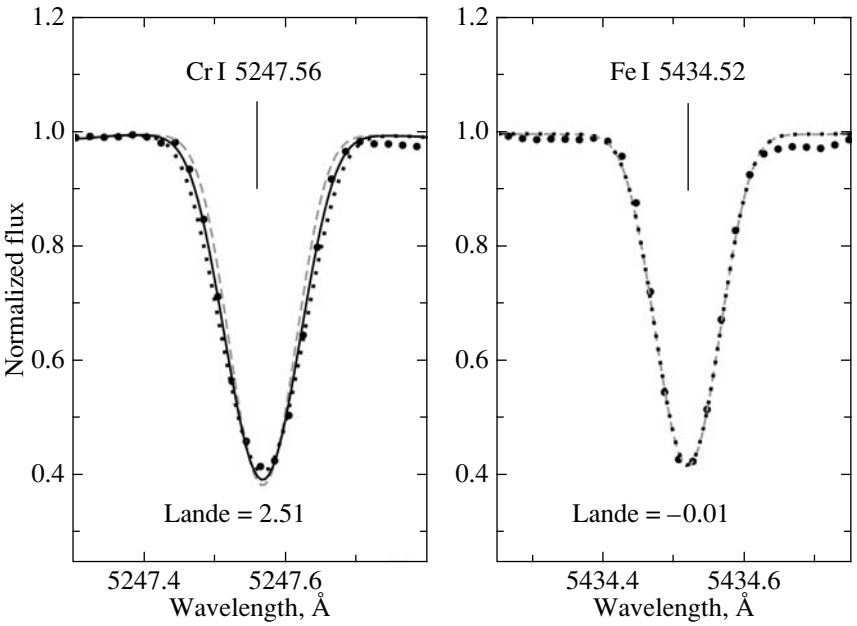

Fig. 1. Magnetic field calculations for HD 138633 as applied to two lines, Cr I 5247.56 Å and Fe I 5434.52 Å. The filled circles mark the points of the observed spectrum, the dashed curve indicates the calculations without a magnetic field, the solid curve indicates the calculations for a field of 0.7 kG, and the dotted curve indicates the calculations for a field of 1 kG. For the Fe I 5434.52 Å line, we performed our calculations in the absence of a magnetic field and for a field of 1 kG, with the two theoretical spectra being coincident.

presence. The filled circles mark the points of the observed spectrum, the dashed curve indicates the calculations without a magnetic field, the solid curve indicates the calculations for a field of 0.7 kG, and the dotted curve indicates the calculations for a field of 1 kG. It can be concluded from the appearance of the Fe I 5434.52 Å line that the magnetic field actually does not affect the line shape and depth, which makes it most suitable for estimating the rotational velocity in magnetic stars. Thus, the line shape is determined by the instrumental profile and stellar rotation. An additional broadening that corresponds to a magnetic field strength of ≈0.7 kG is needed for the Cr I 5247.56 Å line.

Using the BINMAG code (http://www.astro.uu.se/∼oleg/), which allowed the observed and calculated line profiles to be compared at various rotational velocities, we ascertained that the best agreement between the theoretical and observed Fe I 5434.52 Å line profiles was achieved at $v \sin i \approx 2.8$ km s^{-1}. Such a rotational velocity roughly corresponds to the width of the instrumental profile. At $v \sin i = 2.5$ km s^{-1}, the observed profiles were described best by the theoretical ones when our stratification analysis was performed and no significant changes in the behavior of the theoretical spectrum with decreasing rotational velocity were found. We took this value as the star's rotational velocity. The STEREO observations revealed no rotationally induced photometric variability. Since the lines in the spectrum are narrow, we assume the star's rotation period to be long.

The microturbulence is usually determined by the value at which the dependence of the elemental abundance derived from individual lines on their equivalent widths vanishes. We found that the microturbulence lies within the range from 0 to 0.5 km s^{-1}. This suggests the absence of a significant magnetic enhancement of the spectral line intensities, i.e., a small magnetic field strength, which is an additional confirmation of the above field estimate. We chose the microturbulence to be 0.3 km s^{-1} for our subsequent calculations of the chemical composition.

3. CHEMICAL COMPOSITION AND STRATIFICATION OF ELEMENTS IN THE ATMOSPHERE

We identified the lines in the spectrum by comparing the observed and synthetic spectra. The latter was computed with the Synth3 code for the adopted model atmosphere with $T_{\rm eff} = 8200$ K and $\log g = 3.8$. The atomic data for our computation were taken from the VALD database (Kupka et al. 1999). In the observed spectrum of HD 138633, we measured the equivalent widths of more than 600 unblended lines in the range from 4000 to 7000 Å. Based on the measured equivalent widths and the chosen model atmosphere, we

determined the abundances of chemical elements in the atmosphere of HD 138633. For our abundance analysis, we used the 2010 version of the WIDTH code (Tsymbal 1996), in which the hyperfine splitting was taken into account.

Apart from the main list of lines, which gives the names of the elements and their ionization stages, wavelengths, the corresponding excitation energies, oscillator strengths, damping parameters, Lande factors, and central depths of the lines, an additional list is used in this version of the code. It provides the hyperfine structure constants for the energy levels due to the interaction between the magnetic moment of the nucleus and the magnetic field produced by the electronic shell of the atom for a set of spectral lines. The code seeks wavelength coincidences in the main and additional lists. In the case of a coincidence, the hyperfine splitting is calculated. As a result, the theoretical line profile with the hyperfine splitting calculated with the WIDTH_2010 code is the sum of the profiles produced by all hyperfine splitting components. Allowance for the hyperfine splitting turned out to be important for the europium and cobalt abundances. The hyperfine structure constants for these elements were taken from Lawler et al. (2001) and Pickering (1996), respectively.

Apart from our allowance for the hyperfine splitting, we also took into account the isotopic composition for europium. Europium consists of two isotopes, Eu^{151} and Eu^{153}, whose abundance in the solar atmosphere is approximately the same, and we adopt the same isotopic composition in our calculations. The isotopic shifts were taken from Lawler et al. (2001). Simultaneous allowance for the hyperfine splitting and the isotopic composition in the case of europium causes its abundance in the atmosphere of HD 138633 to decrease by 0.25 dex.

We averaged the abundances derived from individual lines of elements/ions and then calculated the standard deviation. The final elemental abundances are given in Table 3. A significance difference in abundances for the lines of one element in different ionization stages can be seen from the Fe I, Fe II, Ca I, Ca II, Si I, Si II, Y I, and Y II lines. In particular, the abundance derived from the lines of the element in the first ionization stage is considerably higher than that deduced from the lines of the neutral element. Only the abundance of Y, for which the situation is directly opposite, constitutes an exception. At the same time, it should be noted that good agreement in abundances is observed from a large number of Cr I and Cr II lines.

In normal stars, a difference in the abundances of an element in different ionization stages suggests an improper choice of the star's atmospheric parameters. In particular, ionization equilibrium for HD 138633 can be achieved by increasing the effective temperature by 1000 K, which disagrees with the photometric data and the observed hydrogen line profiles. In the atmospheres of magnetic peculiar stars, where their slow rotation and magnetic field lead to stabilization of all macro- and micro-motions, the diffusion of chemical elements under the joint action of radiation pressure and gravity (Michaud 1970) produces chemical composition gradients. Therefore, we assumed the existence of a vertical stratification of elements in the atmosphere of HD 138633, i.e., a nonuniform distribution of chemical elements with depth in the atmosphere. This assumption is supported by the low rotational velocity of HD 138633 and the presence of a magnetic field. For a clear confirmation of the existence of a stratification in the stellar atmosphere, we constructed an analog of the curve of growth for Fe II (Fig. 2), where the expression $X = \log(gf\lambda) - (5040/T_{\rm ex})\epsilon_i$ dependent on the oscillator strength and excitation potential was used as the parameter characterizing the line strength. Here, g is the statistical weight of the lower level for the transition under consideration, f is the line oscillator strength, λ is the transition wavelength, ϵ_i is the excitation potential, and $T_{\rm ex}$ is the excitation temperature.

Figure 2 presents the dependences for HD 138633 and 21 Peg, whose effective temperature is considerably higher, 10 400 K. For the latter star, there is no visible correlation between the elemental abundance and the line strength, suggesting the absence of nonuniformity in the atmospheric distribution of the element. For HD 138633, the situation is different—a strong dependence is seen. If this dependence was due to an improper choice of the temperature, then the model with $T_{\rm eff} \approx 9500$ K should be applied in the calculations to eliminate it, which is inconsistent with the observations.

For our stratification analysis, we chose 32 iron lines, 16 calcium lines, 14 silicon lines, and 15 yttrium lines in two ionization stages that are formed in different atmospheric layers. For example, these are the lines with identical oscillator strengths but significantly differing excitation potentials and, conversely, with similar excitation potentials and differing oscillator strengths. In addition, we used the lines in two ionization stages. We performed our stratification analysis based on the observed line profiles using the DDAFIT code written by Kochukhov (2007) in the IDL programming language. In this code, the distribution of an element is approximated by a step function and we find four parameters: the elemental abundance in the lower atmospheric layers, the elemental abundance in the upper atmospheric layers, the position and width of the jump in abundance, and the formal modeling error for each parameter. The

Table 3. Elemental abundances in the atmosphere of HD 138633. The elemental abundances in the atmosphere of β CrB and the solar elemental abundances (Asplund et al. 2005) are given for comparison; n is the number of measured lines

Species	HD 138633		β CrB	Sun
	$\log N/N_{\rm tot}$ (σ)	n	$\log N/N_{\rm tot}$	$\log N/N_{\rm tot}$
C I	−4.15 (0.28)	4		−3.45
Na I	−5.77 (0.22)	4		−5.71
Mg I	−4.03 (0.14)	5		−4.50
Al I	−5.68	1		−5.57
Al II	−4.26 (0.10)	3		−5.57
Si I	−3.98 (0.25)	25		−4.50
Si II	−3.61	1	−4.09	−4.50
Ca I	−5.21 (0.19)	32	−5.10	−5.68
Ca II	−4.91 (0.22)	6		−5.68
Sc II	−9.42 (0.13)	6		−8.87
Ti I	−7.23 (0.07)	2	−6.15	−7.02
Ti II	−7.70 (0.21)	2	−5.86	−7.02
V II	−8.36	1		−8.04
Cr I	−4.08 (0.27)	152	−4.60	−6.37
Cr II	−3.94 (0.20)	181	−4.68	−6.37
Mn I	−5.02 (0.25)	24		−6.65
Mn II	−5.06 (0.22)	28	−5.02	−6.65
Fe I	−4.00 (0.26)	241	−3.92	−4.59
Fe II	−3.55 (0.28)	161	−3.66	−4.59
Co I	−5.70 (0.27)	24		−7.12
Ni I	−6.22 (0.25)	19	−5.41	−5.79
Sr I	−7.67	1		−9.07
Y I	−6.91 (0.19)	9		−9.80
Y II	−7.89 (0.20)	11		−9.80
Zr II	−7.96 (0.15)	2	−8.39	−9.44
Ba II	−10.34 (0.06)	2		−9.91
La II	−9.50 (0.14)	5	−8.35	−10.87
Ce II	−9.02 (0.15)	16	−7.84	−10.46
Ce III	−6.34 (0.33)	6	−5.65	−10.46
Pr III	−10.13	1	−9.35	−11.33
Nd II	−9.60	1	−9.17	−10.54
Nd III	−10.15	1	−8.36	−10.54
Eu II	−9.06 (0.27)	7	−8.28	−11.53
Eu III	−7.18	1	−5.65	−11.53
Gd II	−8.92 (0.12)	2	−7.54	−10.92
Yb II	−9.31	1		−10.96
$T_{\rm eff}$, K	8200 ± 100		8100 ± 70	5777
$\log g$	3.8 ± 0.1		3.9 ± 0.1	4.44
B_s, kG	0.7		5.7	
$v_e \sin i$, km s^{-1}	2.5		3.0	

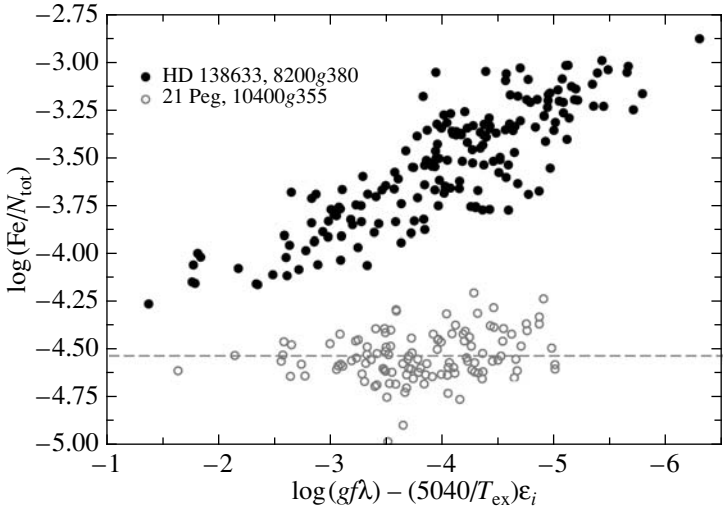

Fig. 2. Curve of growth constructed for Fe for the stars HD 138633 and 21 Peg. For the latter, there is no visible relationship between the elemental abundance and the line strength; for HD 138633, the situation is opposite—the temperature should be increased by 1000 K to eliminate the relationship, which is inconsistent with the observations. The horizontal dashed line indicates the solar iron abundance.

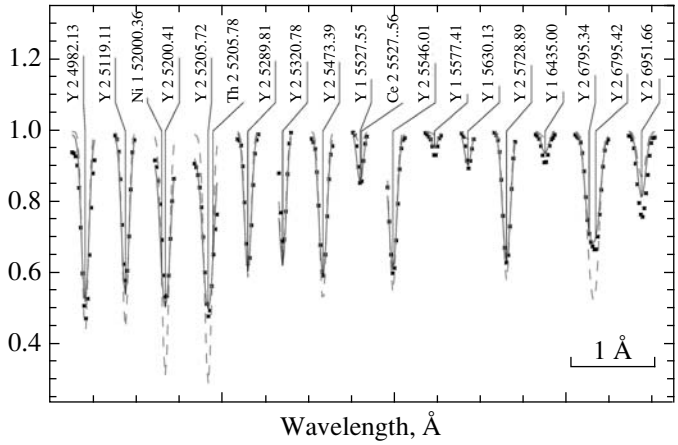

Fig. 3. Comparison of the observed yttrium line profiles in the spectrum of HD 138633 (dotted curve) and the synthetic profiles computed for a chemically homogeneous atmosphere with the abundance from Table 3 (dashed curve) and for a stratified atmosphere (solid curve).

homogeneous abundance from Table 3 was used as the initial approximation.

Figure 3 compares the observed yttrium line profiles and the synthetic profiles computed for chemically homogeneous and stratified model atmospheres. It can be seen from this figure that the observed line profiles can be well described by assuming the atmospheric distribution of elements to be nonuniform. Our stratification analysis yielded an improved model atmosphere in which the distribution of such elements as iron, calcium, silicon, and yttrium is nonuniform. Figure 4 presents the distribution of elements in the atmosphere of HD 138633.

The iron and calcium lines revealed the tendency that the model of a chemically homogeneous atmosphere gives overabundances for the strong lines forming in the upper atmospheric layers and underabundances for the weak lines and the wings of the strong lines forming in the lower atmospheric layers. For silicon, the homogeneous model atmosphere gives an overabundance for all atmospheric layers, to a greater extent for the strong lines forming in the upper atmospheric layers. The yttrium lines revealed the tendency that the homogeneous model atmosphere gives an overabundance for the upper atmospheric layers, where the Y II line cores are formed, and an underabundance for the deep atmospheric layers, where the wings of the strong Y II lines and weak Y I lines are formed. The iron lines revealed the tendency that the homogeneous model atmosphere describes

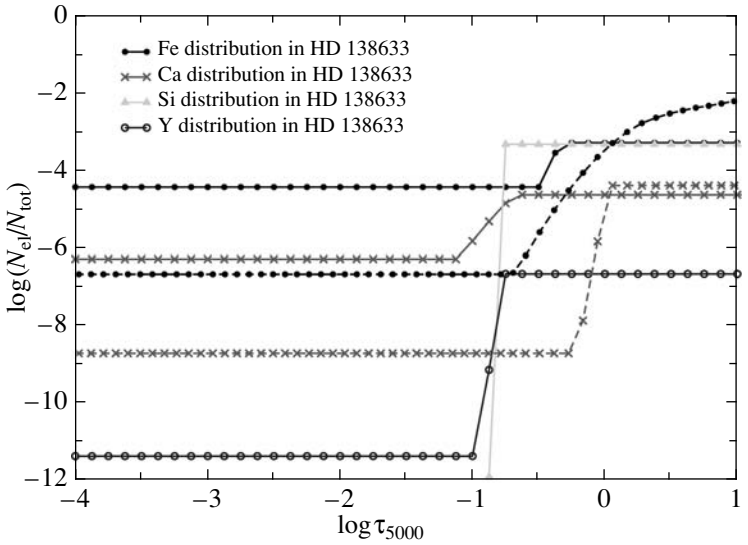

Fig. 4. Distribution of elements in the atmospheres of HD 138633 and β CrB. The solid and dashed curves indicate the distributions of elements in the atmospheres of HD 138633 and β CrB, respectively. The filled circles, crosses, triangles, and open circles correspond to iron, calcium, silicon, and yttrium, respectively.

satisfactorily the line cores, but the abundances for the deep atmospheric layers, where the line wings are formed, are lower than the true ones.

Comparison of the distributions of elements in the atmospheres of HD 138633 and β CrB showed them to agree qualitatively; the difference lies in the positions of the jump in abundances: for β CrB, it is shifted toward deeper atmospheric layers. Qualitatively, this agrees with the predictions of the diffusion theory, according to which the position of the jump in elemental abundance is shifted to higher atmospheric layers with increasing temperature (see Fig. 1 from Ryabchikova (2008)). In addition, as diffusion calculations show, the size of the jump decreases with increasing temperature, which also agrees qualitatively with the results of our comparison of the cooler β CrB and the hotter HD 138633.

4. EVOLUTIONARY STATUS AND VARIABILITY ANALYSIS FOR HD 138633

Since there are no data on the parallax for HD 138633, its luminosity was estimated from evolutionary tracks (Girardi et al. 2000). As a result, we obtained the luminosity $\log(L/L_\odot) = 1.38 \pm 0.2$. This allows the star to be placed on the Hertzsprung–Russell diagram (Fig. 5); it will be in the middle part of the main sequence.

The filled circles mark the subgroup of Ap stars approaching the end of their main-sequence life. There are HD 204411 (Ryabchikova et al. 2005), HD 144897 (Ryabchikova et al. 2006), HD 133792 (Kochukhov et al. 2006), HD 103498 (Joshi et al. 2010), HD 5797, HD 40711 (Semenko et al. 2011), and HD 8441 (Titarenko et al. 2012) in this subgroup. According to the classification by Cowley and Henry (1979), the strong and numerous lines of iron-peak elements in the spectra are typical of this group, while the rare-earth elements are represented very poorly compared to other CP stars. In addition, the stars of this group have weak magnetic fields that are also atypical of Ap stars. Initially, we assumed HD 138633 to belong to this group of stars, but, subsequently, we abandoned this assumption because of the differences in chemical composition and evolution status for HD 138633 and the stars of this group.

The asterisks in Fig. 5 mark the stars with strong magnetic fields with high abundances of both iron-peak and rare-earth elements observed in their spectra. We chose these objects for comparison with the stars from the Cowley–Henry subgroup and, as a result, hypothesized that the stars lose their rare-earth elements during their evolution and their magnetic field decreases. The squares mark the stars to which, as we assume, HD 138633 belongs. Until recently, the stars of this group have not been deemed nonpulsating ones. However, low-amplitude pulsations of β CrB with a period of 16.2 min were found in 2004; at that time, these were among the longest-period pulsations (Hatzes and Mkrtichian 2004). Another star, HD 177765, with the longest known period, 24 min, was discovered in 2012 (Alentiev et al. 2012). In this group of stars, HD 138633 stands out by the presence of a weak magnetic field, while the other two stars have "normal" (strong) fields. The open circles

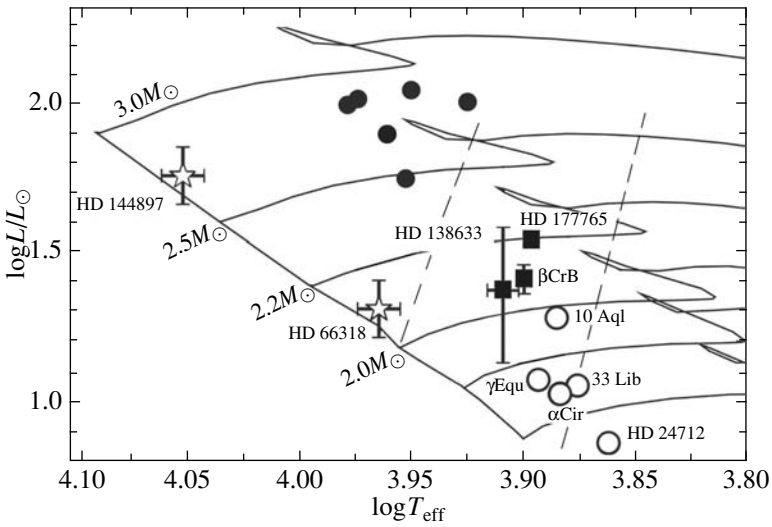

Fig. 5. Hertzsprung–Russell diagram with the marked positions of HD 138633 and the comparison stars. The black circles mark the subgroup of Ap stars to which HD 204411, HD 144897, HD 133792, HD 103498, HD 5797, HD 40711, and HD 8441 belong. The strong and numerous lines of iron-peak elements in the spectra are typical of this subgroup, while the rare-earth elements are represented very poorly compared to other chemically peculiar stars. In addition, the stars of this group have weak magnetic fields that are also atypical of Ap stars. The asterisks designate the stars with strong magnetic fields with high abundances of both iron-peak and rare-earth elements observed in their spectra. We chose these objects for comparison with the stars of the above subgroup and, as a result, we hypothesized that the stars lose their rare-earth elements during their evolution and their magnetic field decreases. The squares mark the group of stars to which, as we assume, HD 138633 belongs. The pulsation period is 16.2 min for β CrB and 24 min for HD 177765. The presumed pulsation period for HD 138633 is 17 min. HD 138633 stands out by the presence of a weak magnetic field, while the other two stars have "normal" (strong) fields. The open circles marks classical roAp stars with pulsation periods of 6–12 min. The oblique dashed lines mark the boundaries of the instability strip.

represent such classical roAp stars with pulsation periods of 6–12 min as α Cir, γ Equ, 10 Agl, 33 Lib, and HD 24712. The theoretically calculated boundaries of the instability strip taken from Theado et al. (2009) are also shown.

We compared the atmospheric chemical compositions of HD 138633 and β CrB. The latter differs in chemical composition from classical roAp stars. Its spectrum exhibits virtually no typical Pr and Nd anomalies (when the elemental abundance from the lines in the second ionization stage exceeds that from the lines in the first ionization stage by one and a half or two orders of magnitude), but, at the same time, the anomalies of other rare-earth elements (Ce and Eu) are observed. In addition, it is strongly anomalous in Fe and Cr abundances. Comparison showed that the stars are similar in chemical composition and atmospheric distribution of elements: large iron and chromium overabundances, no Pr and Nd anomalies, Ce and Eu anomalies are observed. The difference lies in the total abundance of rare-earth elements—in the atmosphere of HD 138663, it is lower than that in β CrB by an order of magnitude, which may be related to a different magnetic field strength.

The similarity of the elemental abundances in HD 138633 and β CrB led us to the decision to perform a more detailed pulsation analysis of HD 138633. Since the pulsations of β CrB were detected from cerium and europium lines, we primarily decided to check the presence of pulsations in HD 138633 based on the lines of the same elements. We measured the radial velocities of 16 Ce II lines and 3 Eu II lines by measuring the position of the line centroid (Kochukhov and Ryabchikova 2001). A peak corresponding to a pulsation period of $\approx$17 min is distinguished in the strongest Eu II 6645 Å line (see Fig. 6). This period is 16.2 min for β CrB. We cannot yet assert that the signal is statistically significant, because this peak is at the 1σ level and appears only in one (strongest) line. The averaged radial velocity curve determined from 16 cerium lines also shows a peak at 16 min, but it is not statistically significant. In any case, even if the pulsations are present, their amplitude does not exceed 30 m s^{-1}. Unfortunately, all cerium lines are too weak for the radial velocity pulsations with such an amplitude to be measured.

5. DISCUSSION AND CONCLUSIONS

A comprehensive analysis of the atmosphere of the chemically peculiar star HD 138633 has been performed for the first time. Using the temperature calibrations for Strömgren photometry and the observed line profiles in the spectrum, we determined

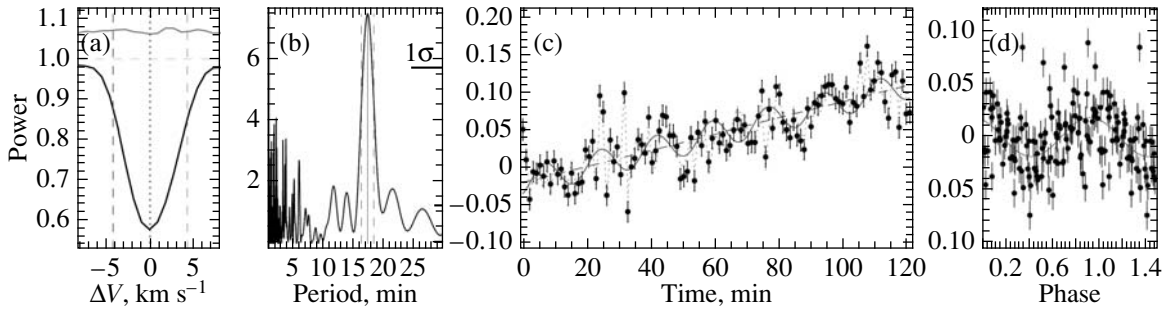

Fig. 6. Pulsations in the atmosphere of HD 138633. (a) The choice of the Eu II 6645 Å line used to search for pulsations. The upper curve indicates the rms deviation of all pulsation spectra from the average spectrum based on which our calculations were ultimately performed. (b) The power spectrum; the horizontal line indicates the 1σ level. (c) The radial velocity variations with time. The dashed line indicates a linear fit whose slope was taken into account in the folding. (d) The radial velocity curve folded with a period of 17 min.

the model atmosphere with $T_{\rm eff} = 8200 \pm 100$ K and $\log g = 3.8 \pm 0.1$. Based on a sample of more than 600 unblended lines, we analyzed the atmospheric chemical composition.

Taking into account the presence of narrow lines and the fact that the star exhibits no rotationally induced variability, we concluded that the star's rotation period is long. Based on on the disturbance of ionization equilibrium for individual elements, such as iron, calcium, silicon, and yttrium, we hypothesized a stratification for these elements in the stellar atmosphere. Our analysis confirmed a nonuniform distribution of elements in the atmosphere. Our estimation of the magnetic field from the differential broadening of spectral lines leads to an upper limit for the magnetic field of 0.7 kG.

Having determined the star's luminosity from evolutionary tracks, we established that HD 138633 belongs to the group of roAp stars in the atmospheres of which pulsations have been detected only recently; β CrB and HD 177765 are present in this group. We found evidence of pulsations with a period of 17–18 min from EuII lines. The presumed pulsation period of HD 138633 agrees with the pulsation period of β CrB, 16.2 min. The pulsation amplitude is 20 ± 4 m s^{-1}, but this error is the formal error of the mean. The resultant error is such that the signal exceeds the 1σ level.

Comparison of the atmospheric chemical compositions of HD 138633 and β CrB shows a high degree of similarity. The differences lie in the abundances of such rare-earth elements as Eu and Ce: their atmospheric abundances in HD 138633 are lower by an order of magnitude, although the rare-earth abundance anomalies for these two stars are similar in pattern. The differences in the abundances of rare-earth elements and stellar magnetic fields led us to the hypothesis that the magnetic field of some peculiar Ap stars weakens during their evolution and, as a consequence, the atmospheric abundances of rare-earth elements are reduced. The question about the relationship between the magnetic field and the abundances of rare-earth elements depending on the mass and evolutionary status of the star remains open at present due to the small number of studied objects.

ACKNOWLEDGMENTS

This study was supported by the Ministry of Education and Science of the Russian Federation (contract no. 8529) and the "Nonstationary Phenomena and Objects of the Universe" Basic Research Program of the Russian Academy of Sciences.

REFERENCES

1. D. Alentiev, O. Kochukhov, T. Ryabchikova et al., Mon. Not. R. Astron. Soc. **421L**, 85 (2012).
2. M. Asplund, N. Grevesse, and A. J. Sauval, ASP Conf. Ser. **336**, 25 (2005).
3. S. Bagnulo, J. D. Landstreet, G. Lo Curto, et al., Astron. Astrophys. **403**, 645 (2003).
4. C. R. Cowley and R. Henry, Astrophys. J. **233**, 633 (1979).
5. L. Girardi, A. Bressan, G. Bertelli, et al., Astron. Astrophys. Suppl. **141**, 371 (2000).
6. A. P. Hatzes and D. E. Mkrtichian, Mon. Not. R. Astron. Soc. **351**, 663 (2004).
7. B. Hauck and M. Mermilliod, Astron. Astrophys. Suppl. **129**, 431 (1998).
8. S. Joshi, T. Ryabchikova, O. Kochukhov, et al., Mon. Not. R. Astron. Soc. **401**, 1299 (2010).
9. A. Kaiser, ASP Conf. Ser. **349**, 257 (2006).
10. O. Kochukhov, in *Physics of Magnetic Stars, Proceedings of the International Conference,* Ed. by D. O. Kudryavtsev and I. I. Romanyuk (Nizhnii Arkhyz, 2007), p. 109.
11. O. Kochukhov and T. Ryabchikova, Astron. Astrophys. **374**, 615 (2001).
12. O. Kochukhov, V. Tsymbal, T. Ryabchikova, et al., Astron. Astrophys. **460**, 831 (2006).

13. F. Kupka, N. E. Piskunov, T. A. Ryabchikova, et al., Astron. Astrophys. Suppl. **138**, 119 (1999).
14. R. L. Kurucz, Kurucz CD-ROM (Smithsonian Astrophysical Observatory, Cambridge, MA, 1993).
15. J. E. Lawler, M. E. Wickliffe, E. A. den Hartog, and C. Sneden, Astrophys. J. **563**, 1075 (2001).
16. F. LeBlanc and D. Monin, in *The A-Star Puzzle, Proceedings of the 224th IAU Symposium,* Ed. by J. Zverko, W. W. Weiss, J. Žižňovský, and S. J. Adelman (Cambridge Univ. Press, 2004), p. 193.
17. G. Michaud, Astrophys. J. **160**, 641 (1970).
18. T. T. Moon and M. M. Dworetsky, Mon. Not. R. Astron. Soc. **217**, 305 (1985).
19. R. Napiwotzki, D. Schönberner, and V. Wenske, Astron. Astrophys. **268**, 653 (1993).
20. J. C. Pickering, Astrophys. J. Suppl. Ser. **107**, 811 (1996).
21. P. Renson and J. Manfroid, Astron. Astrophys. **498**, 961 (2009).
22. F. Rufener, Astron. Astrophys. Suppl. **26**, 275 (1976).
23. T. Ryabchikova, Contrib. Asron. Obs. Skalnate Pleso **38**, 257 (2008).
24. T. Ryabchikova, F. Leone, and O. Kochukhov, Astron. Astrophys. **438**, 973 (2005).
25. T. Ryabchikova, A. Ryabtsev, O. Kochukhov, and S. Bagnulo, Astron. Astrophys. **456**, 329 (2006).
26. E. A. Semenko, I. A. Yakunin, and E. Yu. Kuchaeva, Astron. Lett. **37**, 20 (2011).
27. S. Theado, M.-A. Dupret, A. Noels, and J. W. Ferguson, Astron. Astrophys. **493**, 159 (2009).
28. A. R. Titarenko, E. A. Semenko, and T. A. Ryabchikova, Astron. Lett. **38**, 721 (2012).
29. V. V. Tsymbal, ASP Conf. Ser. **108**, 198 (1996).
30. S. C. Wolff and N. D. Morrison, Publ. Astron. Soc. Pacif. **85**, 141 (1973).
31. K. T. Wraight, L. Fossati, M. Netopil, et al., Mon. Not. R. Astron. Soc. **420**, 757 (2012).

Translated by V. Astakhov